COMMISSIONING OF THE RENEWED LONG RADIAL PROBE IN PSI's RING CYCLOTRON

M. Sapinski*, R. Dölling, M. Rohrer, Paul Scherrer Institut, Villigen, Switzerland

Abstract

PSI's Ring cyclotron is a high intensity proton cyclotron producing a CW proton beam of 2 mA. The beam is accelerated over about 180 turns from 72 MeV to 590 MeV. The Long Radial Probe, called RRL scans the beam along a machine radius over the whole range of turns, i.e. from 2048 mm to 4480 mm. A replacement for the RRL has been developed in the last years. The recently installed new probe drives three carbon fibers with 30 µm diameter through the turns and measures secondary electron emission (SE) currents, providing information on horizontal and vertical beam shape and position. Additional drives are available for a later extension of measurement capabilities. The main challenges are the coupling of the device elements to RF fields leaking from the accelerating cavities, plasma interfering with the measured signal, and the performance of the carbon fibers in a harsh environment with a high-intensity beam and RF heating. We report on the commissioning of the probe with RF and beam and discuss measurement results.

INSTRUMENT DESIGN

The RRL drives three carbon fibers stretched between the upper and bottom trolley, along the radius of PSI's Main Ring cyclotron [1, 2]. The trolleys, powered by the same stepper motor, move synchronously with a speed of 29.7 mm/s. The fibres are oriented vertically and tilted -45° and +45° seen in the beam direction. The setup is visualized in Fig. 2 of [3].

The vertical wire (0°) crosses all orbits in the cyclotron, the -45° wire misses the first orbit and the +45° wire misses the first four orbits. Each scan is performed in two directions: from the parking position at a radius of 4480 mm to the most inner position at 2048 mm (scan *in*) and back (scan *out*).

Between the upper and bottom parts of the main structure of the probe there is a 40 mm clearance for the beam. The structure is milled out of an aluminum alloy (EN AW-5083) and its overall weight is around 100 kg. It contains cables, cable trays, metallic perforated transmission belts used to move the trolleys, and thermocouples to measure the main probe structure temperature. It is grounded at the top and bottom of the vacuum chamber by 20 roller contacts each (Fig. 1). The contacts are installed in pairs, spaced by 25 cm. Four shields are installed on both sides to protect fibres from RF fields and plasma.

Measurement of trolley vibrations performed with PCB-356B18 triaxial accelerometer revealed that the highest vibration amplitude is in the direction of the scan (Fig. 2). The frequency spectrum is broad and drops above 400 Hz, however, it is not yet clear how it affects the signal quality.

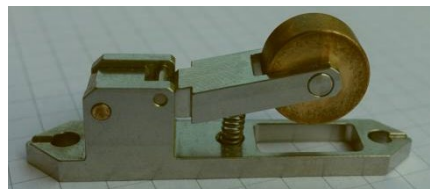

Figure 1: Roller contact for grounding probe structure.

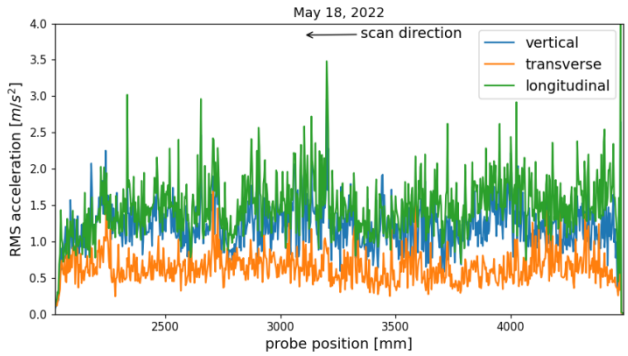

Figure 2: The RMS acceleration measured on the trolley during the scan.

The RRL is installed in the intermediate sector chamber #2, an area of the cyclotron in between two dipole magnets and not equipped with a RF cavity (see Fig. 3 of [2]). This sector contains the electrostatic injection septum EIC and is on the outside equipped with three air-filled ionization chambers called MRI2 at the low radius, MRI9 at the high radius, and MRI9B in the middle.

The signals from the carbon fibers are digitized by MESON logarithmic amplifier modules [4] outside of the bunker, which also control the movement of the trolleys.

COMMISSIONING WITHOUT BEAM

One of the main concerns was the coupling of the RRL structure and the carbon wires to the RF fields leaking out of the cyclotron RF cavities. Therefore, numerous RRL measurements were performed during the RF-conditioning period in March and April 2022.

Observation of RF Heating

Fast detection of eventual strong temperature changes of RRL elements is not possible with the thermocouples due to the large thermal inertia of the main structure. Hence, a FLIR AX8 camera with infrared and visible light sensors has been installed at the height of the machine midplane (Fig. 3). The viewport with a ZnSe IR-transparent window was mounted on a specially-designed flange with an angle allowing for optimal coverage of the probe structure. This flange was equipped with RF shields due to concerns about

* e-mail address: mariusz.sapinski@psi.ch

RF field influence on the camera. Finally, no such influence has been observed during the succeeding measurements. In the course of the RF conditioning, the FLIR camera was set up to register images every few seconds. An example is shown in Fig. 4. An additional camera, SONY SNC-RX570P, was mounted on a second viewport. It provided additional imaging and remotely-controlled illumination, as IR imaging has been done in dark, with all bunker lights off.

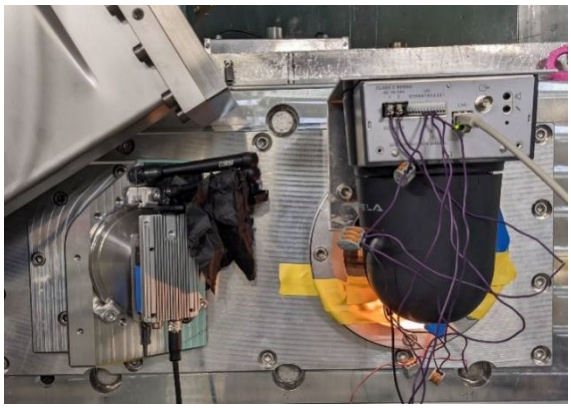

Figure 3: FLIR camera (left) and Sony camera. The RRL is on the left, outside of the frame. (A fragment of the vacuum valve, separating the RRL probe chamber from the machine vacuum, is visible in the upper left corner.)

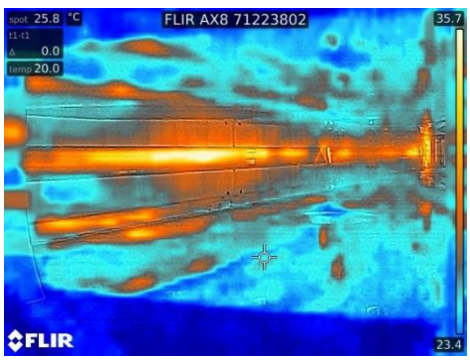

Figure 4: Image produced by the FLIR camera in mixed mode, where both, IR sensor and visible spectrum image are overlapped. The temperature scale is not corrected for viewport transmission. The three wires /\| are apparent.

No fast temperature changes of structure parts have been observed during commissioning. At regular RF operation the main probe structure stayed below 40 °C. However, with one of the 50 MHz RF cavities (#3) accidentally switched off, the thermocouples indicated heating of the main probe structure at a rate of 12 °C/hour. Uninterrupted, this may result in temperatures above 100 °C and hence we will interlock this.

The carbon fibers are glowing due to heating by the RF coupling to it. The temperature could not be measured by the IR sensor because of its limited spatial resolution. However, the glowing was also apparent in visible light as seen in Fig. 5. The vertical wire exhibits the strongest glow. This wire broke at a scan done with RF cavity #3 switched off, i.e. at stronger RF input. At replacement of this wire, the readback cable was disconnected at the wire mount. The decreased capacitance already resulted in a weaker glowing. In addition, we will install isolators with lower permittivity in the wire mounts. Measurement of the -45° wire resistance during the scan shows a decrease from 4.4 kΩ at the parking position down to 3.4 kΩ in the middle of the scan. The temperature estimated from the drop of resistivity is reaching 1130 K (Fig. 6).

Figure 5: Carbon fibres glowing in visible spectrum due to excitation by RF field leaking from RF cavities.

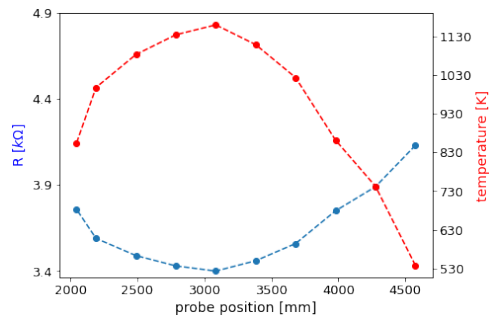

Figure 6: Wire resistance in various probe positions. Estimation of wire temperature based on resistance temperature coefficient $-5 \cdot 10^{-4}$ [1/K] and active wire length 56 mm.

Interaction with Electrostatic Injection Septum

The RRL is measuring the very first beam orbit, right after the EIC, which operates with a static voltage of 140 kV. No effect of the presence of the RRL on the HV and dark current of EIC has been observed.

However, when later scanning high-intensity beams, an increased number of beam interlocks due to EIC HV trips have been noticed. Interestingly those interlocks take place mainly during the scan out. Possibly dust particles from the bottom of the chamber are transported towards the EIC, provoking sparks.

COMMISSIONING WITH BEAM

The first measurements with the beam took place on April 27th, 2022. The IR camera, which survived weeks of operation in the presence of RF fields and gamma rays from multipacting electrons, suffered radiation damage and stopped working after receiving an approximate flux of about $2.5*10^5$ neutrons/cm^2. However, no dead pixels were

observed and the radiation damage most likely occurred in camera electronics.

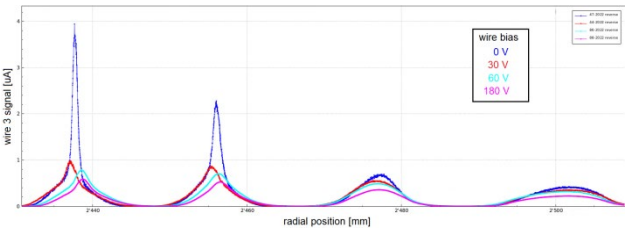

Figure 7: Effect of wire biasing. The four turns seen by the +45° wire are differently affected by TE due to the different beam current densities caused by different horizontal and vertical beam sizes. As always, wire positions at midplane height are corrected for the relative wire positions in the probe head.

The high power density input by the beam in addition to the RF-heating leads to the occurrence of a strong thermionic emission (TE) when the wire crosses the beam. At full beam current, the TE signal can be several times higher than the SE signal at a wire potential of 0 V. A bias voltage of 30 V, applied to the wires, suppresses the TE to a high degree, while the SE is much less affected. At higher bias voltages the TE and SE are further suppressed, but comparatively strong (Fig. 7). The difference at lower bias voltage may be explained by the counteracting effect of the bunch space-charge potential which is present at the creation of all SE but only of a low percentage of TE [5].

An example of a profile registered by the vertical wire at a test beam with reduced intensity is depicted in Fig. 8. At larger machine radii, orbits overlap leading to difficulties in the determination of the peaks. This is especially challenging at high beam intensity. Turn separation is an important parameter of a cyclotron. It is shown in Fig. 9. Figures 7 and 8 have been obtained at special injection settings, which should result in reduction of vertical beam oscillations. This centered beam setting can only be used with reduced beam intensity, because of high relative beam losses.

Figure 10 zooms on the profiles registered by all three wires at inner machine radii. The relative position of the peaks measured by vertical and tilted wires can be used to compute the vertical positions of the turns [6], as shown in Fig. 11. The oscillations of the vertical beam position from orbit to orbit are expected [7], however a large bump at low energies up to about 130 MeV is still being investigated.

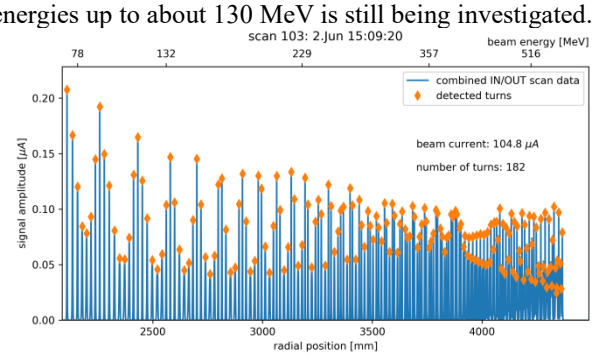

Figure 8: Profile from 0° wire performed at special injection settings (centred beam) with wire bias 60 V.

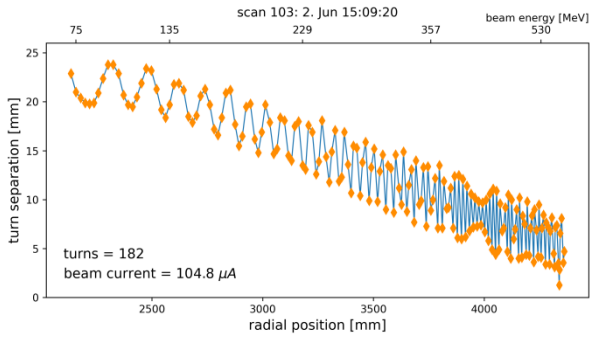

Figure 9: Turn separation derived from 0° wire peak positions as a function of machine radius (The peak finding algorithm has a problem at large radii). The blue line is a guide for the eye.

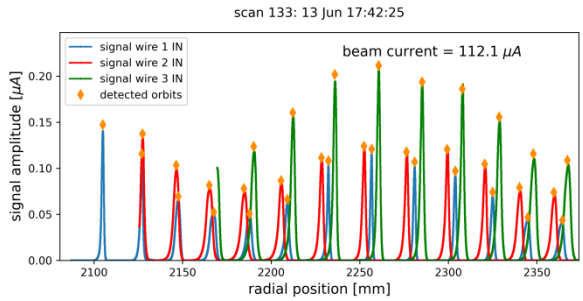

Figure 10: Signals of 0°, -45°, +45° wires. (Wire bias 60 V.)

The position of this bump (r=2500 mm) approximately coincides with an activation hot spot of the probe structure of about 1 mSv/h, discovered after about one month of RRL presence inside the cyclotron. The Monte-Carlo simulations using MNCP [8] revealed that the observed activation could be generated by a loss of the primary beam of the order of 5 nA per meter of machine radius. However, the loss could be generated on a carbon collimator upstream with a narrower gap. The simulation indicates that the activation will not increase in the long term if the probe structure stays in the sector chamber only for the monthly beam development shifts. Motorization of the probe insertion is underway to provide this. However, also the beam loss mechanisms in the Ring cyclotron and the role of the carbon collimators have to be better understood to lower the beam losses in the cyclotron in general.

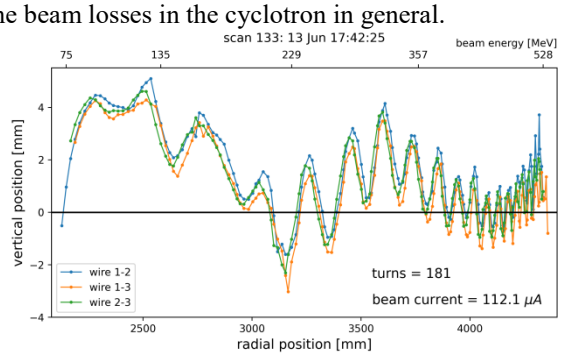

Figure 11: Vertical position of the beam obtained from comparison of wire signals. Due to uncertainties in the vertical position of the probe, the absolute values of measured beam position may be offset or tilted.

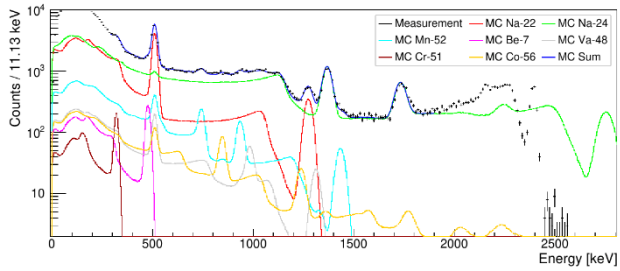

Figure 12: Gamma-ray spectrum at the hot spot [9].

Figure 12 shows the gamma spectrum measured in the location of the hot spot using portable spectrometer BRAD and fitted using contributions from expected radioisotopes. The measured spectrum is closest to the simulated contributions from various radioisotopes assuming proton energy in the range 60-80 MeV, what suggests that the activation is caused by scattered beam.

The vertical oscillations are affected by the injection angle and trim coils. Measurements of the vertical oscillations have been performed changing injection angle and trim coils. A correlation between the amplitude of the vertical bump at r=2500 mm and the signal in the MRI2 chamber has been found. This indicates that the presence of the vertical bump leads to increased beam losses, however, the increased loss does not have to be due to RRL presence.

The vertical and the +45° wire broke at a later point, surprisingly without significant thermal load. These events will be studied by analyzing the wires' remnants with electron microscope to maximize wire reliability.

CONCLUSIONS

The main Ring Cyclotron long radial probe has been renewed and the 3-wire scan brought to operation. It already provided valuable measurements, but there are still issues that have to be addressed. Besides activation and TE, these issues are the increased number of EIC trips during the scan, survival of the carbon fibers exposed to strong RF fields and vibrations, and signal noise. Therefore the ongoing developments include, e.g., further study of the configuration of the RF shields, internal cable quality, lower wire diameters and improved wire mounting. In parallel, the extension of measurement capabilities by equipping the additional drives with, e.g., loss monitors and phase probes will be pursued.

ACKNOWLEDGEMENTS

The authors would like to thank R. Senn and S. Lindner for assembling the probe, R. Senn for contributing to the design of the drag chain support, J. Bachmann for flange design, J. Snuverink for adapting the probe driving software, I. Besana for MNCP calculations, X. Wang and P. Hottinger for performing the noise measurement, M. Hauenstein for activation measurements, E. Hohmann for providing the gamma-ray spectrometer, D. Werthmüller for Gamma-ray spectrum evaluation, E. Yukihara and L. Bossin for precise dosimetry, R. Kan for providing the Sony camera and organizing bunker works, H. Zhang and C. Baumgarten for discussions, beam dynamics simulations and setting up beam centred beam used to obtain Figs. 8 and 9.

REFERENCES

[1] M. Seidel *et al.*, "Production of a 1.3 MW proton beam at PSI", in *Proc. IPAC'10*, Kyoto, Japan, May 2010, paper TUYRA03, pp. 1309-1313.

[2] R. Dölling *et al,* "Development of a replacement for the Long Radial Probe in the Ring Cyclotron", in *Proc. Cyclotrons'19*, Cape Town, South Africa, Sep. 2019, pp. 86-89. doi:10.18429/JACoW-Cyclotrons2019-MOP024

[3] R. Dölling, E. Johansen, M. Roggli and M. Rohrer, "Progress of Profile Measurement Refurbishment Activities at HIPA", in *Proc. IBIC'20,* Santos, Brazil, Sep. 2020, pp. 179-183. doi:10.18429/JACoW-IBIC2020-WEPP33

[4] E. Johansen, "VME Meson design specification", PSI, Villigen, Switzerland, Jun. 2010, unpublished.

[5] R. Dölling, "Bunch-shape measurements at PSI's high-power cyclotrons and proton beam lines", in *Proc. Cyclotrons'13*, Vancouver, Canada, Sep. 2013, paper TU3PB01, pp. 257-261.

[6] L. Rezzonico *et al.*, "Diagnostics for high intensity beams", in *Proc. BIW'94,* Vancouver, Canada, Oct. 1994, *AIP Conf. Proc.,* vol. 333, pp. 398-494, 1995. doi:0.1063/1.48013

[7] C. Baumgarten, H. Zhang, private communication, Jun. 2022.

[8] M. I. Besana and J. Snuverink, "Activity simulations for long probe RRL", unpublished report, Aug. 2022.

[9] D. Werthmüller, private communication, Jul. 2022